Carbohydrate Polymers 174 (2017) 1181–1191

Contents lists available at ScienceDirect

Carbohydrate Polymers

journal homepage: www.elsevier.com/locate/carbpol

Effect of moderate electric fields in the properties of starch and chitosan films reinforced with microcrystalline cellulose

Caroline C.S. Coelho[a,b,c,*], Miguel A. Cerqueira[d], Ricardo N. Pereira[c], Lorenzo M. Pastrana[d], Otniel Freitas-Silva[b], António A. Vicente[c], Lourdes M.C. Cabral[a,b], José A. Teixeira[c]

[a] PPGCAL/Instituto de Química, UFRJ, Cidade Universitária, Ilha do Fundão, CEP: 21949-900 Rio de Janeiro, RJ, Brazil
[b] Embrapa Agroindústria de Alimentos, Av. das Américas, 29501, 23.020-470, Rio de Janeiro, RJ, Brazil
[c] Centre of Biological Engineering, Universidade do Minho, Campus de Gualtar, 4710-057, Braga, Portugal
[d] International Iberian Nanotechnology Laboratory, Av. Mestre José Veiga s/n, 4715-330, Braga, Portugal

ARTICLE INFO

Article history:
Received 11 April 2017
Received in revised form 20 June 2017
Accepted 3 July 2017
Available online 4 July 2017

Keywords:
Cellulose
Electric field
Electro-heating
Biopolymer
Edible coating
Packaging

ABSTRACT

Microcrystalline cellulose (MCC) can provide improved properties when the aim is the development of biodegradable packaging materials. In this work the physicochemical properties of polysaccharide-based films (chitosan and starch) with the incorporation of MCC and the application of moderate electric field (MEF) and ultrasonic bath (UB) as treatments, were evaluated. For each treatment, the thickness, moisture content, solubility, water vapor permeability, contact angle, mechanical properties, along with its color and opacity were determined. The surface morphologies of the films were assessed by scanning electron microscopy (SEM). X-ray diffraction (XRD), Fourier-transform infrared (FTIR) spectroscopy and thermogravimetric analysis (TGA) were also performed. It was observed that the addition of different concentrations of MCC as well as the application of MEF are responsible for changes in the properties of the films, being this effect dependent on the polysaccharide used. Chitosan-based films were slightly yellow, transparent and presented a more homogeneous structure. The use of MEF was efficient in decreasing the permeability to water vapor in chitosan based films without MCC, as well as in production of films with a more hydrophobic surface. The addition of MCC promoted more opaque, rigid, less flexible and less hydrophobic films. Starch-based films were whitish, with a more heterogeneous structure and the application of MEF generated more hydrophilic films with lower tensile strength and Young's modulus. The films with MCC were more opaque, less flexible and less hydrophilic than the films without MCC. The composites presented good thermal properties, which increases their applicability as packaging materials. Therefore, the incorporation of MCC into polysaccharide-based films as well as the application of MEF can be an approach to change the properties of films.

1. Introduction

Recently, the demand for products made from sustainable resources with renewable and biodegradable features has become an important part of the effort to reduce the impact of food packaging on the environment (Souza et al., 2010) being used to reduce the amount of synthetic materials in the food chain. In this context, edible films based on biopolymers, as chitosan and starch, appear as potential substitutes of petroleum-based packaging materials, because of their abundant and renewable availability, non-toxic, low cost, biodegradable and biocompatible nature (Dehnad et al., 2014; Shankar & Rhim, 2016; Souza et al., 2009; Shi et al., 2013). However, the development of packaging materials is still a challenge (Rico, Rodríguez-Llamazares, Barral, Bouza, & Montero, 2016).

Studies reported that incorporation of microcrystalline cellulose (MCC) can be done as a compatible reinforcing filler for biopolymers (Ma, Chang, & Yu, 2008; Rico et al., 2016). The incorporation of MCC in starch and chitosan-based films appears particularly interesting due to the chemical similarities in the polysaccharide structure, which can lead to a good interfacial adhesion of the matrix-cellulose, which is crucial to improve mechanical and barrier properties of the developed composites (Celebi & Kurt, 2015;

* Corresponding author at: PPGCAL/Instituto de Química, UFRJ, Cidade Universitária, Ilha do Fundão, CEP: 21949-900 Rio de Janeiro, RJ, Brazil.
E-mail address: carolcsc@hotmail.com (C.C.S. Coelho).

http://dx.doi.org/10.1016/j.carbpol.2017.07.007
0144-8617/

Rico et al., 2016). In this way, ensure that MCC is homogeneously dispersed within the film matrix, it is a challenge that has been achieved by using ultrasonic technologies such as ultrasonic bath (UB) (Slavutsky & Bertuzzi, 2014). Therefore, the search for new methodologies for the preparation of biocomposites should be addressed aiming improved film properties. One of the proposals is the use of electro-heating technology that is also known as moderate electric fields (MEF). It is based on the passage of electric current through a sample having an inherent electric resistance, where the electrical energy is converted directly into heat and the instantaneous heating occurs at a rate which depends on the intensity of the current passing through the material (Pereira, Souza, Cerqueira, Teixeira, & Vicente, 2010; Souza et al., 2010). This technology has been used in several applications in food processing as in operations of blanching, evaporation, dehydration and pasteurization (Sastry & Barach, 2000). Recently, it gained a new interest in the food area being applied in film production of proteins and polysaccharides (Pereira et al., 2010; Souza et al., 2010). There are some studies showing significant improvement of various properties of edible films and coatings with the application of moderate electric fields (MEF) (García, Famá, Dufresne, Aranguren, & Goyanes, 2009; Lei, Zhi, Xiujin, Takasuke, & Zaigui, 2007; Pereira et al., 2010; Souza et al., 2009, 2010). Nevertheless, there are still no studies on the application of this technology in chitosan and starch filmogenic solutions with the incorporation of MCC.

Thus, this study aimed to produce chitosan and starch-based films with incorporation of different concentrations of MCC and evaluate the effects of incorporation under MEF and UB treatments. Physical and structural characterization of the produced films, as well as the effect of the different MCC concentrations on the film properties were also addressed.

2. Materials and methods

2.1. Materials

Starch potato was obtained from Sigma-Aldrich Química, S.L (Portugal), and a high molecular weight and deacetylated (95%) chitosan was obtained from Golden-Shell Biochemical Co., Ltd. (Yuhuan, China). Glycerol (87%) was obtained from Acros Organics (Belgium), lactic acid (98 %) was obtained from Merck (Germany), and microcrystalline cellulose (MCC) (Avicel® PH-101, 11363; density is 0.26–0.31 g/cm^3, particle size is approximately 50 μm and the moisture content vary in the range of 3–5%) was obtained from Sigma-Aldrich Química, S.L (Portugal).

2.2. Film preparation

The starch film (ST) forming solution was prepared by mixing starch (1%, w/v) and water. The chitosan- based film (CH) solutions were prepared by dissolving the chitosan (1%, w/v) in a 1% (v/v) lactic acid solution. Both solutions were stirred using a magnetic stirrer at 400 rpm for 21 h at room temperature (20 °C); subsequently an appropriate amount of MCC was added to the solution (0.1 or 0.2%, w/v). Then, the mixture was left under stirring for 2 h and the glycerol added at a concentration of 0.25 g/g$_{polymer}$ and left under agitation for 1 h. Two treatments were performed to the film forming solutions, heating with further dispersion in sonication bath and moderate electric fields.

2.2.1. Ultrasonic bath

The ST and CH film-forming solutions (prepared as was described in Section 2.2) were heated in a shaking water bath at 70 °C during 30 min under agitation (400 rpm). This procedure ensured the total dissolution of ST and CH and the formation of a homogeneous dispersion. Temperature progress, during conventional experiment, was measured with a thermocouple, placed at the geometric center of the sample volume. The resulting dispersion was kept 45 min in ultrasonication bath (UB) (Branson 5510 Ultrasonic Cleaners, Frequency: 40 kHz), used to disperse 0.1 and 0.2% of MCC in the matrix, which were named as CH.UB-0.1, ST.UB-0.1, CH.UB-0.2, ST.UB-0.2, respectively. Samples that did not contain MCC were entitled CH.UB-C or ST.UB-C. At the end, a constant amount of the film-forming solutions (28 mL) were cast in acrylic plates (90 mm × 15 mm) and dried at 35 ± 1 °C for 24 h in an air-circulating oven.

2.2.2. Moderate electric fields

A set of experiments was conducted to determine the effect of using moderate electric fields (MEF) on the production of CH and ST –based films with 0.1 and 0.2% MCC (CH.MEF-0.1 or ST.MEF-0.1 and CH.MEF-0.2 or ST.MEF-0.2, respectively). Samples that did not contain MCC were entitled CH.MEF-C or ST.MEF-C.

The heater used consisted of a cylindrical glass tube of 30 cm total length and 2.3 cm inside diameter; two Titanium electrodes with Teflon pressure caps placed at each end of the tube.

The CH film forming solution samples (prepared as was described in Section 2.2) were treated using a MEF intensity of 7.6 V cm^{-1} with an interval of 6 cm between the electrodes, which allowed working at constant temperature of 70 °C. A magnetic stirrer was introduced inside the glass tube to homogenize the solution and improve heat transfer during the heating cycle. Temperature was controlled using of a function generator (Agilent 33220A, Penang, Malaysia) connected to amplifier equipment (Peavey CS3000, Meridian, MS, USA) and alternating current source with an electrical frequency of 25 kHz. Temperatures were monitored using a type-K thermocouple (1 °C, Omega, 709, USA), placed at the geometrical center of the chamber through an available opening. A data logger (National Instruments, USB-9161, U.S.A.) working with Lab View 7 Express software (National Instruments, NI Data logger) was employed to record continuously treatment temperature. Electrical frequency, voltage applied and current intensity were measured simultaneously using portable oscilloscope (ScopeMeter® 125/S, 124 Fluke, Everett, WA, USA).

The same conditions were used for the ST film forming solution (according described in Section 2.2), but due to its low electrical conductivity, the experiments were performed in a double-walled water-jacketed reactor vessel (3 mm of internal diameter and 100 mm height) connected to temperature controlled water bath (~70 °C). This allowed working at the same electric field as CH solution, without changing thermal conditions.

2.3. Characterization of the films

2.3.1. Conditioning

All dried films were stored in desiccators at 25 °C and 54% relative humidity (obtained using a $Mg(NO_3)_2{\cdot}6H_2O$-saturated solution) until tests. The moisture content, solubility, water vapor permeability and thermogravimetric analysis measurements were performed in triplicate.

2.3.2. Thickness

Film thickness was measured with a hand-held digital micrometer (No. 293-561, Mitutoyo, Japan). Thickness measurements were taken on each testing sample in ten different randomly chosen points and the mean values were used for water vapour permeability and mechanical properties determination.

2.3.3. Moisture content

The moisture content was determined gravimetrically using Eq. (1), by drying the films at 105 °C in an oven with forced air circulation for 24 h.

$$MC(\%) = \frac{Mt - Mf}{Mt} \times 100 \quad (1)$$

Where M_i and M_f are the masses of initial and dried samples, respectively. The experiments were performed in triplicate, and expressed as the percentage of water removed from the initial mass sample.

2.3.4. Film solubility

The measurement of film solubility (Sol) in water was determined according to the method reported by Cuq, Gontard, Cuq, & Guilbert (1996), by immersion in water of dried films using Eq. (2).

$$Sol(\%) = \frac{Mi' - Mf'}{Mi'} \times 100 \quad (2)$$

Where M_i' is the initial mass, M_f' is the final mass of the sample and *Sol* represent the percentage of film solubility.

Triplicates of each film were cut with a circular mold of 2 cm diameter, dried at 105 °C in an oven for 24 h and weighed. Then the samples were immersed in 50 mL of water, sealed with parafilm and stirred in an orbital shaker at 60 rpm for 24 h at 25 °C. The non-soluble part of each film was taken out and dried at 105 °C in an oven for 24 h and weighed again in order to determine the weight of dry matter.

2.3.5. Water vapor permeability measurement (WVP)

The measurement of water vapor permeability (WVP) of the films was determined gravimetrically based on the ASTM E96-92 method (Guillard, Broyart, Bonazzi, Guilbert, & Gontard, 2003; McHugh, Avenabustillos, & Krochta, 1993).

The film was sealed on the top of a permeation cell containing distilled water (100% RH; 2337 Pa vapour pressure at 20 °C) and placed in a desiccator at 20 °C and 0% RH (0 Pa water vapor pressure) with silica gel. The cups were weighed at intervals of 2 h during 10 h. The water transferred through the film and adsorbed by the desiccant was determined from weight loss of the permeation cell. Steady-state and uniform water pressure conditions were assumed by keeping the air circulation constant outside the test cup by means of a miniature fan placed inside the desiccators (McHugh et al., 1993). The slope of the curve representing the weight loss versus time was obtained by linear regression.

2.3.6. Contact angle

Contact angle measurements were performed in a face contact angle meter (OCA 20, Dataphysics, Germany). The samples of the films were taken with a 500 μL syringe (Hamilton, Switzerland), with a needle of 0.75 mm of diameter. The contact angle at the film surfaces was measured by the sessile drop method (Kwok & Neumann, 1999). Each measurement was made within 10 s. At least fifteen contact angle measurements were obtained for each sample at 19.8 (±0.3) °C.

2.3.7. Optical properties

The color of films was determined with a digital Minolta colorimeter (Konica Minolta, model Chroma Meter CR-400, Osaka, Japan). The CIELab scale was used to determined L^*, a^* and b^* color parameters (Alparslan, Baygar, Baygar, Hasanhocaoglu, & Metin, 2014). The opacity (*Y*) was determined as the relationship between the opacity of each sample on a black standard (Y_b) and the opacity of each sample on the white standard (Y_w) (Casariego et al., 2009), using Eq. (3).

$$Y(\%) = \frac{Yb}{Yw} \cdot 100 \quad (3)$$

Where Y_b is the black standard and Y_w is the white standard. Samples were analyzed in triplicate, recording five measurements for replicate.

2.3.8. Scanning electronic microscopy (SEM)

The effect of MCC incorporation in film was evaluated in respect to the surface morphology and cross-sectional using scanning electron microscope (SEM) (Nova NanoSEM 200, Eindhoven, Netherlands) with an accelerating voltage of 10 a 15 kV under vacuum conditions. Before analyses, the films were maintained at 20 °C and 54% relative humidity (RH) for 24 h. All samples were mounted on aluminum stubs using carbon adhesive Tape, and after that were sputter-coated with gold with thickness of about 10 nm.

2.3.9. Mechanical properties

Tensile strength (TS), elongation at break (EB) and Youngís modulus (YM) were measured with a TA.HD plus Texture Analyzer (Serial RS232, Stable Micro Systems, Surrey, UK), with a load cell of 5 kg, following the guidelines of ASTM D 882-02 (2010). Film strips with a length of 120 mm and a width of 20 mm were used and the average film thickness was measured with digital micrometer (Section 2.3.2). The initial grip separation was set at 100 mm and the crosshead speed was set at 5 mm min^{-1}. The tests were replicated nine times for each sample.

2.4. X-ray diffraction (XRD)

X-ray diffraction patterns of the samples were analyzed between $2\theta = 4°$ and $2\theta = 60°$ with a step size $2\theta = 0.02°$ in an X-ray diffraction instrument (Bruker D8 Discover, USA).

2.5. Fourier-transform infrared (FTIR) spectroscopy

The films were characterized by Fourier Transform Infrared (FTIR) Spectroscopy on a Bruker FT-IR VERTEX 80/80 v (Boston, USA) in Attenuated Total Reflectance mode (ATR) with a platinum crystal accessory between 400 and 4000 cm^{-1}, using 16 scans at a resolution of 4 cm^{-1}. Before analysis, an open bean background spectrum was recorded as a blank. The neat films of chitosan and starch were used as control and each spectrum recorded for the films with the incorporation of MCC and different treatments.

2.6. Thermogravimetric analysis (TGA)

Thermogravimetric analysis (TGA) was completed with a PerkinElmer TGA 4000 (PerkinElmer, Massachusetts, EUA). For TGA analysis about 10–12 mg of the sample were placed in the balance system and heated from 20 °C to 450 °C at a heating rate of 10 °C min^{-1} under a nitrogen atmosphere.

2.7. Statistical analysis

One-way ANOVA was applied to analyze data and when detected the existence of significant differences between treatments, the averages were compared according to the Tukey test, adopting the 5% ($\alpha = 0.05$) significance level. The statistical analyses were performed using SISVAR version 5.6 program (SISVAR®, Brazil).

3. Results

3.1. Thickness, moisture content, solubility, water vapour permeability and contact angle

Table 1 shows the values of thickness, moisture content (MC), solubility (Sol), water vapour permeability (WVP) and contact angle (CA) of the chitosan-and starch based films with increasing concentrations of MCC and the UB and MEF treatments.

The incorporation of MCC in the chitosan- based films increased ($p < 0.05$) the film thickness for both treatments, with no differences observed between treatments using UB and MEF. The MC values of the neat chitosan film decrease significantly ($p < 0.05$) when 0.2% of MCC was added to the films (CH.UB-0.2) ($28.20 \pm 0.01\%$). However, for films treated with MEF such results were not observed, and the incorporation of MCC in chitosan-based films showed no effect ($p > 0.05$). For film solubility, no significant differences ($p > 0.05$) were observed among all treatments.

The application of MEF lead to lower WPV values for chitosan control films (CH.MEF-C), being these values statistically different from the other treatments ($p < 0.05$). This behavior was not observed when MCC was incorporated in the chitosan-based films (CH.MEF-0.1 and CH.MEF-0.2).

The hydrophilicity of films can be accessed through the determination of the contact angle between a water drop and the film surface. In order to understand the effect of MCC and treatment (i.e. MEF and UB) on films hydrophilicity, contact angles were determined for all the produced films. Results showed that when MCC is added to chitosan-based films, the CA values decreased (CH.UB-0.1, CH.UB- 0.2, CH.MEF-0.1 and CH.MEF-0.2) when compared to the respective control films (CH.UB-C and CH.MEF-C). However, the CA values were higher when the MEF treatment was applied, forming more hydrophobic films (CH.MEF-C, CH.MEF-0.1 and CH.MEF-0.2) (Supporting information Fig. 1).

In the starch-based films the ST.UB-0.1 and ST.UB-0.2 films showed higher thickness values (0.058 and 0.081 mm, respectively), that result from the addition of MCC in the films matrix. The same behavior was observed for the chitosan-based films; however, the thickness values were lower when the MEF treatment was applied.

The MC of the starch-based film increased significantly ($p < 0.05$) when 0.1% of MCC was incorporated in the films, regardless of the applied treatment (ST.UB-0.1 and ST.MEF-0.1). Solubility of starch-based films with or without addition of MCC and regardless of the treatment applied (UB or MEF) was not statistically different ($p > 0.05$).

The results showed that ST.UB-0.1 and ST.UB-0.2 films are more permeable ($p < 0.05$) when compared to the ST.UB-C films and to the films where MEF was applied (ST.MEF-C, ST.MEF-0.1, ST.MEF-0.2). Therefore, the ST.UB-C, ST.MEF-C, and ST.MEF-0.2 films presented lower WPV values. For starch-based films, the incorporation of 0.1% MCC leads to significantly higher CA values ($p < 0.05$). When the MEF treatment was applied, the CA values decreased significantly ($p < 0.05$) and thus leading to the formation of more hydrophilic films (ST.MEF-C, ST.MEF-0.1 and ST.MEF-0.2) (Supporting information Fig. 1).

3.2. Optical properties

Table 2 shows the color parameters and opacity values for chitosan and starch-based films. For the consumer, the films should be visually attractive, in order to maintain the acceptance of the product when applied (Souza et al., 2009). As shown in Table 2, in CH films, the lightness (L), a^* and b^* values did not change significantly ($p < 0.05$) after incorporation of MCC and the applied treatments (UB or MEF).

All the films with MCC were perceived to be slightly opaque (Table 2 and Supporting information Fig. 2) but only chitosan-based films with 0.2% MCC (CH.UB-0.2 and CH.MEF-0.2) exhibited significantly higher ($p < 0.05$) values of opacity when compared to the control film (CH.UB-C and CH.MEF-C, respectively).

In starch-based films the results show that the lightness is somewhat high ($p < 0.05$) with addition of MCC and application of MEF treatment (ST.MEF-0.1 and ST.MEF-0.2). The a^* values did not change significantly after incorporation of MCC as well as was not affected by the applied treatments (UB or MEF). The increase of b^* indicates the intensification of the yellowness of the starch-based film. The increase of b^* values of both treatments with MCC films were observed, regardless of the treatment applied (UB or MEF). However, there were no significant differences in b^* between ST.UB-0.1 and ST.UB-C films ($p > 0.05$). This result shows that the application of MEF in films with MCC had a significant effect on L* and b^* parameters of starch films.

As well as the chitosan- based film, all the starch films with the addition of MCC were perceived to be slightly opaque (Table 2 and Supporting information Fig. 2). Starch-based films with 0.2% and 0.1% MCC (ST.UB-0.1, ST.UB-0.2, ST.MEF-0.1 and ST.MEF-0.2) exhibited significantly higher ($p < 0.05$) values of opacity when compared to the control film (ST.UB-C and ST. MEF-C).

3.3. Scanning electron microscopy

SEM was used to evaluate the morphology of the films before and after incorporation of MCC and after the use of UB and MEF treatments. As can be seen in Fig. 1a, SEM micrograph of control chitosan-based film (CH.UB-C and CH.MEF-C) shows a relatively smooth surface without any phase separation indicating an appropriate dissolution of chitosan in the acidic solution (Dehnad et al., 2014).The chitosan- based films containing different concentrations of MCC showed a more heterogeneous Surface (Fig. 1(a) CH.UB-01, CH.UB-0.2, CH.MEF-0.1 and CH.MEF-0.2). This observation was also verified with the analysis of the cross-sectional images, where some visible changes were noticed when compared with the control film. It is clear that the roughness of the surface of the films increases when MCC is added to the starch-based film, these results can be seen in Fig. 1. It can also be noted that the application of the MEF treatment has formed starch-based films with more MCC in the surface, this fact can be noticed both on the surface of the film (Fig. 1(a) – ST.UB-01, ST.UB-0.2, ST.MEF-0.1 and ST.MEF-0.2) as well as in the cross-sectional image (Fig. 1(b) – ST.UB-01, ST.UB-0.2, ST.MEF-0.1 and ST.MEF-0.2).

3.4. Mechanical properties

Table 3 presents the TS, EB and YM values of chitosan and starch-based films. For the chitosan films, the addition of MCC was not effective to increase the TS. The use of MEF treatment in the preparation of films increased the TS in CH.MEF-C when compared to the CH.UB-C ($p < 0.05$). EB values decreased for film with higher MCC content, namely for CH.UB-0.2, CH.MEF-0.1 and CH.MEF-0.2 with exception of the CH.UB-0.1 film. An inverse relationship was found for the YM values, once these films had the highest values of YM. However, for the films with MEF treatment the EB values were only reduced in case of CH.MEF-0.1 when compared to the CH.UB-C ($p < 0.05$), while YM values remained unchanged.

Regarding the starch-based films, the addition of MCC in both concentrations lead to a decreasing of the TS values for UB films ($p < 0.05$). This pattern was different from the behavior observed for the chitosan- based films, where the application of MEF treatments resulted in films with lower TS, with or without MCC. The films with MCC showed lower values of EB but with application of MEF treatment in the starch solution, the ST.MEF-C and ST.MEF-

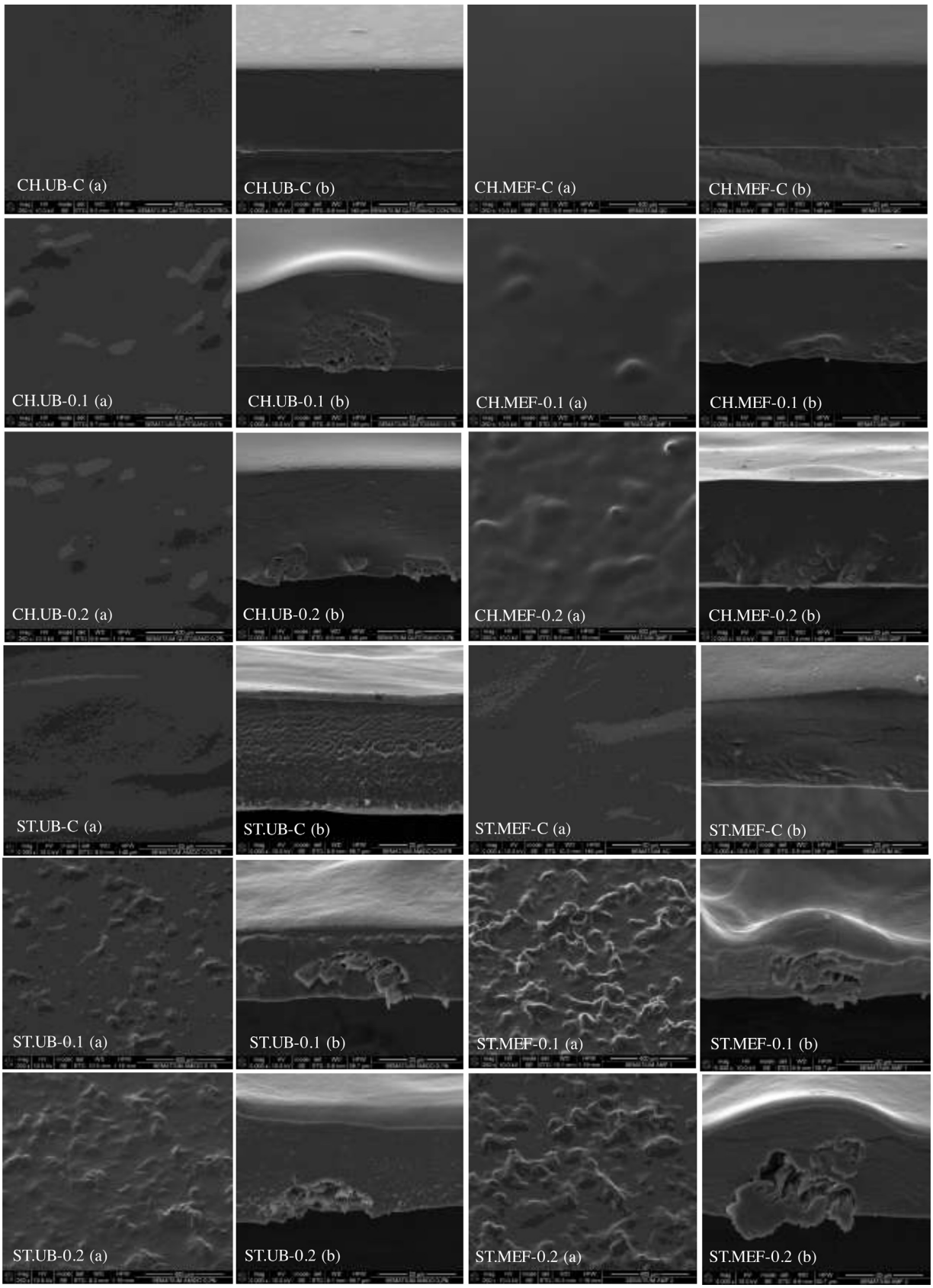

Fig. 1. Scanning electron microscopy images of (a) surface at 250× of magnification with scale bar of 400 μm and (b) cross-sectional at 2000× of magnification with scale bar of 50 μm for chitosan-based films(CH) and cross-sectional at 5000× of magnification with scale bar of 20 μm for starch-based films (ST) films without and with addition of MCC after treatment with ultrasound bath (UB) and moderate electric fields (MEF).

Table 1
Values of thickness, moisture content (MC), solubility (Sol), water vapor permeability (WVP) and contact angle (CA) of the chitosan (CH) and starch (ST) based films with different microcrystalline cellulose (MCC) concentrations (0.1 or 0.2%) after ultrasound bath (UB) or moderate electric fields (MEF) treatments.

Film	Thickness (mm)	MC (%)	Sol (%)	WVP × 10^7 (g h^{-1} m^{-1} Pa^{-1})	CA (°)
CH.UB-C	0.069 ± 0.005^{a}	36.56 ± 0.02^{a}	35.95 ± 0.03^{a}	2.26 ± 0.17^{a}	71.94 ± 1.47^{a}
CH.UB-0.1	0.090 ± 0.002^{b}	41.14 ± 0.01^{a}	33.48 ± 0.03^{a}	2.60 ± 0.05^{a}	64.52 ± 1.59^{b}
CH.UB-0.2	0.094 ± 0.002^{b}	28.20 ± 0.01^{b}	30.25 ± 0.03^{a}	2.57 ± 0.08^{a}	51.44 ± 1.96^{c}
CH.MEF-C	0.064 ± 0.008^{a}	39.70 ± 0.03^{a}	34.04 ± 0.04^{a}	1.68 ± 0.16^{b}	103.29 ± 3.60^{d}
CH.MEF-0.1	0.084 ± 0.004^{b}	39.43 ± 0.02^{a}	32.09 ± 0.01^{a}	2.19 ± 0.24^{a}	91.62 ± 0.48^{e}
CH.MEF-0.2	0.091 ± 0.004^{b}	37.33 ± 0.01^{a}	30.32 ± 0.01^{a}	2.38 ± 0.15^{a}	75.87 ± 2.44^{a}
ST.UB-C	0.047 ± 0.002^{AB}	12.04 ± 0.02^{A}	23.06 ± 0.03^{A}	1.43 ± 0.13^{A}	41.68 ± 1.82^{A}
ST.UB-0.1	0.058 ± 0.003^{C}	22.08 ± 0.01^{B}	20.00 ± 0.01^{A}	2.19 ± 0.20^{B}	50.62 ± 1.38^{B}
ST.UB-0.2	0.081 ± 0.001^{D}	10.64 ± 0.02^{A}	20.67 ± 0.03^{A}	2.51 ± 0.06^{B}	48.70 ± 1.36^{B}
ST.MEF-C	0.039 ± 0.009^{A}	12.45 ± 0.04^{A}	23.45 ± 0.07^{A}	1.12 ± 0.25^{A}	24.94 ± 0.84^{C}
ST.MEF-0.1	0.044 ± 0.003^{AB}	28.90 ± 0.01^{B}	18.09 ± 0.03^{A}	1.81 ± 0.16^{C}	31.14 ± 1.04^{D}
ST.MEF-0.2	0.047 ± 0.002^{B}	12.91 ± 0.05^{A}	21.588 ± 0.01^{A}	1.24 ± 0.08^{A}	28.68 ± 0.57^{CD}

Different letters in the same column indicate a statistically significant difference ($p < 0.05$), where lowercase letters correspond to chitosan-based films samples and uppercase letters correspond to starch-based films.

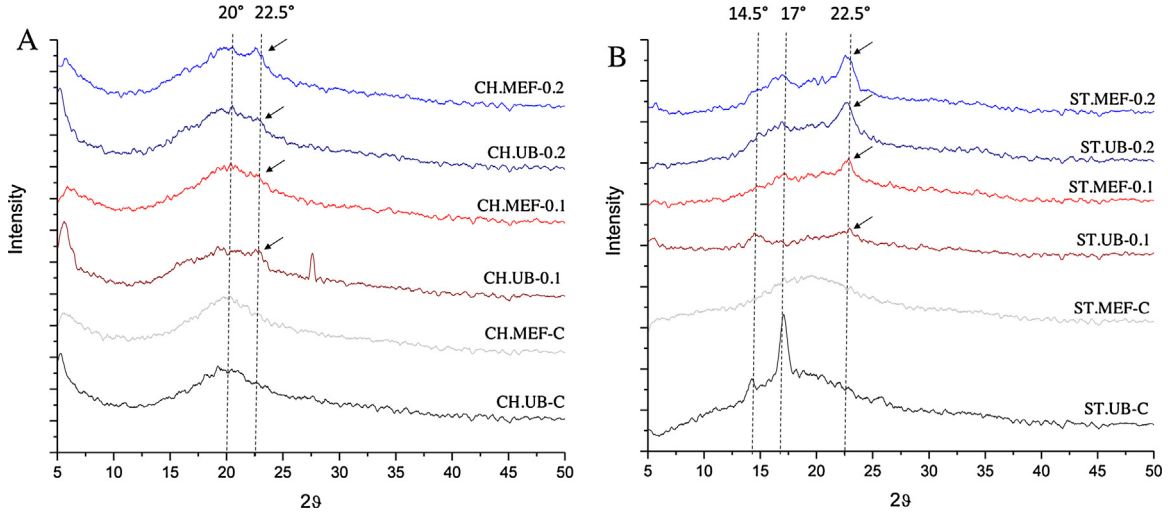

Fig. 2. Diffractograms of chitosan (A) and starch (B) based films with different microcrystalline cellulose (MCC) concentrations (0.1 or 0.2%) after ultrasound bath (UB) or moderate electric fields (MEF) treatments.

Table 2
Optical properties of chitosan (CH) and starch (ST) based films with different microcrystalline cellulose (MCC) concentrations (0.1 or 0.2%) and ultrasound bath (UB) or moderate electric fields (MEF) treatments.

Film	L* (lightness)	a*	b*	Opacity (%)
CH.UB-C	94.52 ± 0.16^{a}	-1.38 ± 0.29^{a}	14.09 ± 3.24^{a}	4.07 ± 0.62^{a}
CH.UB-0.1	94.49 ± 0.18^{a}	-1.20 ± 0.12^{a}	13.14 ± 0.64^{a}	5.50 ± 0.43^{ab}
CH.UB-0.2	94.69 ± 0.38^{a}	-1.03 ± 0.19^{a}	11.66 ± 1.07^{a}	9.06 ± 2.20^{c}
CH.MEF-C	94.09 ± 0.52^{a}	-1.26 ± 0.15^{a}	13.05 ± 1.31^{a}	4.87 ± 0.78^{a}
CH.MEF-0.1	94.25 ± 0.68^{a}	-1.19 ± 0.11^{a}	12.88 ± 1.63^{a}	6.75 ± 1.96^{abc}
CH.MEF-0.2	94.32 ± 0.64^{a}	-0.95 ± 0.08^{a}	11.50 ± 1.17^{a}	8.40 ± 0.21^{bc}
ST.UB-C	97.11 ± 0.16^{A}	0.19 ± 0.01^{A}	1.97 ± 0.05^{AB}	9.74 ± 0.19^{A}
ST.UB-0.1	97.47 ± 0.11^{A}	0.16 ± 0.04^{A}	2.08 ± 0.01^{BC}	12.46 ± 0.27^{B}
ST.UB-0.2	97.39 ± 0.05^{A}	0.13 ± 0.02^{A}	2.14 ± 0.08^{C}	13.25 ± 0.13^{B}
ST.MEF-C	97.20 ± 0.29^{A}	0.15 ± 0.04^{A}	1.86 ± 0.04^{A}	10.06 ± 0.46^{A}
ST.MEF-0.1	98.12 ± 0.19^{B}	0.21 ± 0.10^{A}	2.03 ± 0.05^{BC}	12.80 ± 0.43^{B}
ST.MEF-0.2	98.08 ± 0.20^{B}	0.17 ± 0.02^{A}	2.04 ± 0.03^{BC}	14.15 ± 1.21^{B}

Different letters in the same column indicate a statistically significant difference ($p < 0.05$), where lowercase letters correspond to chitosan-based films samples and uppercase letters correspond to starch-based films.

Table 3
Mechanical properties of chitosan (CH) and starch (ST) based films for increasing microcrystalline cellulose (MCC) concentrations for ultrasound bath (UB) or moderate electric fields (MEF) treatments.

Film	Tensile strength (MPa)	Elongation at break (%)	Young's modulus (MPa)
CH.UB-C	3.05 ± 0.40^{a}	108.21 ± 2.13^{a}	0.02 ± 0.01^{a}
CH.UB-0.1	4.40 ± 0.41^{ab}	112.55 ± 1.97^{a}	0.04 ± 0.02^{ab}
CH.UB-0.2	4.95 ± 0.43^{abc}	64.40 ± 2.29^{b}	0.09 ± 0.02^{cd}
CH.MEF-C	7.36 ± 1.39^{d}	106.78 ± 15.54^{a}	0.05 ± 0.01^{abc}
CH.MEF-0.1	5.55 ± 0.45^{bcd}	63.94 ± 2.78^{b}	0.08 ± 0.01^{bcd}
CH.MEF-0.2	6.77 ± 0.84^{cd}	72.19 ± 6.16^{b}	0.10 ± 0.01^{d}
ST.UB-C	31.70 ± 1.33^{A}	3.07 ± 0.17^{A}	14.51 ± 1.25^{A}
ST.UB-0.1	14.70 ± 1.58^{B}	1.84 ± 0.23^{B}	10.78 ± 0.50^{B}
ST.UB-0.2	14.05 ± 1.22^{B}	1.95 ± 0.04^{B}	9.65 ± 1.0^{B}
ST.MEF-C	7.31 ± 0.53^{C}	4.81 ± 0.19^{C}	3.85 ± 0.83^{C}
ST.MEF-0.1	6.42 ± 0.16^{C}	2.96 ± 0.26^{AD}	4.08 ± 0.46^{C}
ST.MEF-0.2	5.86 ± 1.19^{C}	2.28 ± 0.46^{BD}	4.14 ± 0.90^{C}

Different letters in the same column indicate a statistically significant difference ($p < 0.05$), where lowercase letters correspond to chitosan-based films samples and uppercase letters correspond to starch-based films.

0.1 films showed higher EB values when compared to ST.UB-C and ST.UB-0.1 films ($p < 0.05$). The YM was affected by all concentrations of MCC increment in the matrix when UB treatment was applied (ST.UB-0.1 and ST.UB-0.2), decreasing the values of YM ($p < 0.05$). The application of MEF treatments resulted in films with lower YM, with or without MCC.

3.5. X-ray diffraction (XRD)

Structural analysis of chitosan and starch-based films with and without MCC, after UB and MEF treatment was performed by XRD.

Fig. 2 represents the diffractograms of the CH and ST-based films, after UB and MEF treatment. These patterns are typical of semi-crystalline materials with an amorphous region and crystalline peaks.

The XRD diffractograms showed a reflection peak located at about $2\theta = 22.5^{\circ}$, which is related to the crystalline structure of cellulose I (Segal, Creely, Martin, & Conrad, 1959) This peak can be observed for all films with the increase of MCC content (0.1 or 0.2%). In addition, happens an increase of the peak intensity with increased concentrations of MCC.

In Fig. 2a the CH films peaks were evidenced at $2\theta = 20^{\circ}$, indicates the semi-amorphous nature of this polymer and is in agreement with other published results (Celebi & Kurt, 2015; Dehnad et al., 2014; Souza et al., 2010). The effect of preparation method on XRD can be investigated and no significant changes were observed in the chitosan-based films.

As shown in Fig. 2b, starch films displayed a β-type with strongest reflections at about $2\theta = 17^{\circ}$ and a few smaller reflections at about $2\theta = 14.5^{\circ}$, similar to that reported by Tibolla, Pelissari, & Menegalli (2014) and Li et al. (2016). This can be noticed mainly in the sample ST.UB-C presented strongest reflections in these peaks. The diffraction peak about $2\theta = 17^{\circ}$ decrease in intensity in the other films, and the reflections at about $2\theta = 14.5^{\circ}$ disappeared when the filmogenic starch solutions were treated with MEF. Thus, the application of the MEF changes the diffraction pattern in the starch, and it is not possible to visualize the peaks that are notorious in the samples treated by UB.

3.6. FTIR spectroscopy

Fourier transform infrared spectroscopy (FTIR) was used for the evaluation of possible chemical interactions between MCC and the film matrix (CH and ST) as well as the treatments applied (UB and MEF) and possible modifications in their chemical structure; when compounds are mixed, physical bonds and chemical interactions are reflected by changes in characteristic spectral peaks (Martins, Cerqueira, & Vicente, 2012). Fig. 3a shows a comparison between the FTIR spectra of the CH films with or without MCC after treatment with UB and MEF. The spectra recorded for the films with MCC (CH.UB-0.1, CH.UB-0.2, CH.MEF-0.1 and CH.MEF-0.2) were subtracted to the spectrum obtained for CH control film, according to treatments applied. In general, all of the films presented a broad band between 3500 and 3100 cm^{-1}, attributed to the stretching of hydroxyl (OH) groups that overlaps the N—H stretching vibration in the same region (Celebi & Kurt, 2015; Khan et al., 2012).

The broad band between 2800 and 3000 cm^{-1} is attributed to C—H stretching (Cerqueira et al., 2012; Martins et al., 2012; SriBala, Chennuru, Mahapatra, & Vinu, 2016). With the incorporation of MCC and MEF treatment was observed a low variation in this band. The addition of 0.2% MCC increased the intensity of the bands, while a different behavior was observed for 0.1% MCC, where the intensity of the O—H stretching vibration was similar to the chitosan- based film used as control and all the films UB. The peak approximately at 1733 cm^{-1} is reported to be characteristic of a carbonyl group (C=O) vibrations, present in the film matrix (Pawlak & Mucha, 2003; Martins et al., 2012).

The FTIR spectrum of neat chitosan-based films showed the characteristic saccharide structure peaks at 1030 and 1076 cm^{-1} due to the C single bond O stretching and O single bond H bending, respectively (Celebi & Kurt, 2015; Khan et al., 2012).

Fig. 3b shows a comparison between the FTIR spectra of the ST films with or without MCC after submission of the filmogenic solution to the UB and MEF; the spectra of the ST-based film control was used background. In general, all of the films presented a broad band between 3500 and 3100 cm^{-1}, attributed to the stretching of hydroxyl (OH) groups that overlaps the N—H stretching vibration in the same region. The broad band between 2800 and 3000 cm^{-1} is attributed to C—H stretching vibration (Cerqueira et al., 2012; Martins et al., 2012; SriBala et al., 2016).

With the application of UB treatment was observed a low variation in this band with an increase of the bands intensity. The bands in the region between 1002 and 917 cm^{-1} observed in all spectra were assigned to C—OH deformation of starch molecules and methods related to the CH_2 group. These bands were also identified in the spectra of films with MCC.

3.7. Thermal analyses

Fig. 4a and b shows the peak values and the corresponding weight loss for each event, for CH and ST films, respectively. Thermal analysis shows that for both polymers (CH and ST films) are present at least three thermal events. However, for samples with MCC a fourth event was observed. Small differences are observed in Peak 2 arising from MCC content in the CH-based films, with a decrease of the weight loss in films with 0.2% of MCC (CH.UB-0.2 and CH.MEF-0.2) when compared with the others CH films. There was no difference in the thermal behavior between the treatments applied either UB or MEF.

The thermogravimetric curves of starch films subjected to the different treatments (Fig. 4b) showed essentially the same behavior, indicating that apparently occurs a similar degradation mechanism with the temperature. In ST films containing MCC, the weight loss at peak 1 presents statistically significant differences ($p < 0.05$) where a decrease of the weight loss for the film with 0.2% MCC (ST.UB-0.2 and ST.MEF-0.2) is observed (data not shown). However, these samples do not exhibit a significantly different value when compared with ST.UB-0.1 (5.57 ± 0.50, 5.45 ± 0.41 and 6.29 ± 0.78, respectively) ($p > 0.05$). The difference in weight loss due to the presence of glycerol (peak 2) is also marked, where a decrease of the weight loss for the film with 0.2% MCC (ST.UB-0.2 and ST.MEF-0.2) is observed; nevertheless, these values are not significantly different values from the ST.UB-0.1 and ST.UB-C ($p > 0.05$) (data not shown).

The peak 3 shows that the addition of 0.1% of MCC increases the thermal stability, where a decrease of the weight loss for the film ST.MEF-0.1 ($p < 0.05$) is observed.

4. Discussion

The studied materials are proposed for short-lived applications such as food packaging. For this reason, its behavior at temperatures close to ambient temperature is interesting. The incorporation of MCC in chitosan- based films and starch increased ($p < 0.05$) film thickness, results that are in agreement with published works (Shankar & Rhim, 2016). Also the use of MEF instead of UB treatment in starch-based films presents an effect on films thickness (higher values). Regarding chitosan-based films the type of pretreatment does not change the values that is in agreement with Souza et al. (2010) that showed that the thickness of chitosan-based films produced with the use of electric fields (100 V cm^{-1} and 200 V cm^{-1}) did not show statistical differences ($p > 0.05$) when compared to the untreated samples.

It was also observed that the addition of MCC changed the MC values, being the effect dependent on the biopolymer used. The interaction between the starch molecules (0.1% MCC) produced a greater number of sites available for binding water, so these films showed superior moisture when compared to other starch films. The decrement of the MC content showed by of the chitosan film filled with 0.2% of MCC can be explained by the better dispersion of the higher concentration of the particles promoted by UB treat-

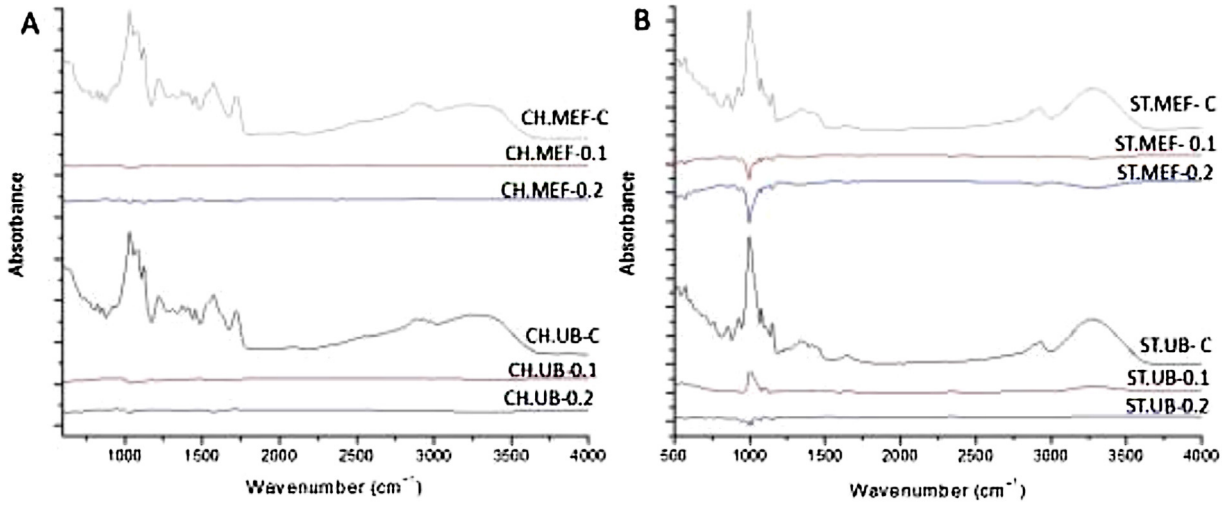

Fig. 3. FTIR spectra of chitosan (A) and starch (B) based films for increasing microcrystalline cellulose (MCC) concentrations after ultrasound bath (UB) or moderate electric fields (MEF) treatments.

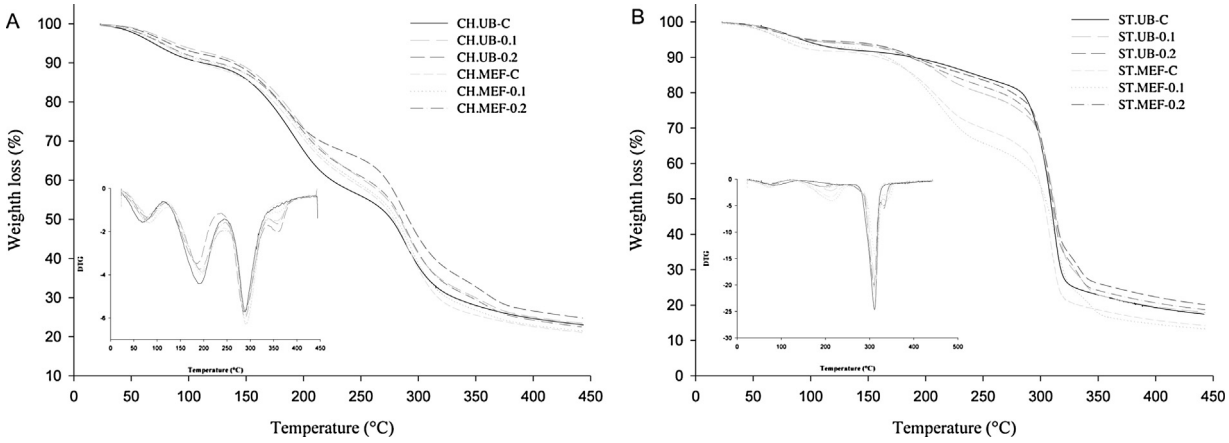

Fig. 4. Thermogravimetric analysis (TGA) and derivative thermogravimetric (DTG) curves for chitosan (a) and starch (b) based films with different microcrystalline cellulose (MCC) concentrations (0.1 or 0.2%) after ultrasound bath (UB) or moderate electric fields (MEF) treatments.

ment, thus the formation of hydrogen bonds between the polymers reduced the interaction between the water and the film.

Some authors have reported that poor dispersion of strengthening material can lead to the formation of agglomerates of such material, even in low concentration, create some preferential route for moisture transport, which facilitates the WVP. Shankar & Rhim (2016) showed that the incorporation of MCC in agar films resulted in increased WVP values which may be due to the bulky structure of MCC. This was also showed in this work when MEF was applied in chitosan-based films, since only the control films showed a decrease of WVP. This in agreement with results obtained by Souza et al. (2010) that showed that WVP of chitosan-based films decreased with increasing field strength values of 100 V cm^{-1} and 200 V cm^{-1}. Regarding the production of starch-based films containing MCC, application of MEF resulted in thinner films. Starch films with MCC produced under effects of MEF presented lower WVP, this result may be associated with smaller thickness of these films.

The CA of the films is a good indicator of the degree of hydrophilicity and hydrophobicity of film surface. According to the Slavutsky & Bertuzzi (2014), an increase in the contact angle indicates an increase in film hydrophobicity. Quantitative differentiation between "hydrophobic" and "hydrophilic" surfaces is based on whether the water contact angle is $\theta > 90^{\circ}$ or $\theta < 90^{\circ}$, respectively (Ma, Hu, Wang, & Wang, 2016). Therefore, all samples of starch films can be considered to have hydrophilic surfaces, presenting values of contact angle below 90°, and chitosan-based films CH.MEF-C and CH.MEF-0.1 can be considered to have hydrophobic surfaces, both presenting values of contact angle above 90°; these results not being observed for other chitosan- based films. MCC is a hydrophilic material, with the presence of hydroxyl groups on their surface (Thoorens, Krier, Leclercq, Carlin, & Evrard, 2014). In chitosan-based films, adding MCC reduces CA values, forming more hydrophilic films. This might be attributed to the hydrophilic character of cellulose particles (Reddy & Rhim, 2014). However, for starch films this result was different, as adding MCC made films less hydrophilic. Slavutsky & Bertuzzi (2014) observed a high increment of the hydrophobic character in starch films when they were added with cellulose nanocrystals (CNC) obtained from sugarcane bagasse; according to authors these indicate a strong interaction between starch chains and CNC with formation of hydrogen bonds reducing the interaction between water and the film surface. In these cases, the differences can be related with the high crystallinity of CNC when compared with MCC that still presents a high amorphous pattern (Bondeson, Mathew, & Oksman, 2006; Li et al., 2009).

The CA values which lead us to conclude that the presence of MEF changes the way that the polysaccharides structure is distributed in the films. Electrical disturbance of MEF can impose reorientation of molecules was described elsewhere (Pereira et al., 2016). In this case, these events may have reduced the exposure of hydrophilic groups. While for chitosan it seems that MEF promotes the reorientation of molecules and reduces the exposure of hydrophilic groups in the surface, for starch films the lower CA values indicate that happens an increase of the exposure of hydrophilic groups toward the surface.

SEM of the chitosan- based films showed a homogeneous and random distribution of the MCC, without pores or cracks, with few visible changes compared with the control film and the heterogeneous structure of the starch film. Most of the particles are embedded rather than pulled out from the chitosan matrix showing a strong interfacial adhesion between the fillers and matrix, as was observed by (Celebi & Kurt, 2015). Apparently, the MCC were covered by the chitosan matrix, showing a good adhesion between both. A more homogeneous dispersion of MCC limits the formation of agglomerates of the material and promotes the cellulose-chitosan interactions needed to ensure the voltage transfer in enhancing interface polymer/matrix.

It is clear that the roughness of the surface of the films increases when MCC are added to the starch-based film. This suggests that the increase of MCC concentrations modified the surface microstructure of the starch-based films, probably due to low compatibility between MCC and starch. The application of the MEF treatment has formed starch films with more MCC in the surface, which could also explain the lower values found for CA.

The addition of the MCC leads to an increase of b^* values of both treatments in starch-based films, which indicates the intensification of the yellowness of the starch film, possibly by MCC color, similar results were obtained when MCC was incorporated into agar matrix (Shankar & Rhim, 2016). All the films presented high values of lightness ($L^* > 94.09$), evidencing the light color.

The addition of MCC leads to more opaque films. The possible reason for higher opacity values in films containing microparticles is due to the fact that mean particle size is much larger than the size of the interspace in matrix film (Shi et al., 2013) and when the light passes through these films, much lower extent of light is transmitted through the film. Thus, this property could be interesting for food packaging as a barrier against light, which is one of the causes of degradation of certain foods.

The addition of the highest MCC concentration studied (0.2%) to chitosan-based films lead to more rigid films when compared to control films. This is explained by the incorporation of MCC that causes a reinforcement of the matrix attributed to the good filler-matrix adhesion, how was observed in SEM morphologies, which is expected to cause an efficient stress transfer from the matrix to the filler (Rico et al., 2016). However, these films showed to become less flexible, meaning lower values of EB. Generally, the incorporation of microcrystals tends to reduce the elongation of the films (Freire et al., 2008; Lu, Weng, & Cao, 2005). Application of MEF changed TS films only when comparing the control films. Thus, such films have higher ability to withstand tensile stress. Souza et al. (2010) observed an increase of TS values for chitosan-based film with MEF treatments of 100 V cm^{-1} and 200 V cm^{-1}.

In starch films, the incorporation of MCC decreased rigidity and resistance capacity under TS in UB films regardless of the concentration used. However, when the starch film-forming solutions were subjected to application of MEF these values were lower, possibly this event can be associated with poor dispersion of microcrystals between the film, as noted in SEM images. As reported in some studies, homogeneous dispersion in the matrix determines the effectiveness of the polymer reinforcing material (Azeredo et al., 2009). The addition of MCC films decreased EB, but the application of MEF provided control films more flexible at 0.1%, i.e. with higher values of EB.

Chuayjuljit, Su-Uthai, Tunwattanaseree, & Charuchinda (2009), reported that the TS of the natural rubber latex sheet reinforced with MCC was affected by poor dispersing of MCC in the matrix when the concentration was too low or too high. This suggests that there is a concentration point for MCC for each type of polymer matrix in which it is possible to obtain a good dispersion of the reinforcing material, which reflects an improvement in mechanical strength material. The particle size is another factor which influences the effectiveness of the reinforcing material, and the smaller particle size have a greater surface area, which enhances its ability to interact with the components of the polymeric matrix for transferring mechanical force (Eichhorn et al., 2010). Thus, the heterogeneity of sizes of MCC observed in SEM (data not shown) may be limiting its capacity as a reinforcing material for these films.

The increase in diffraction peak at $2\theta = 22.5^\circ$ with the addition of MCC in CH and ST films suggests an increase in the crystallinity of films with MCC, consistent with other published works where this phenomenon was attributed to the crystalline nature cellulose derivatives, such as MCC (Ma et al., 2005; Tibolla et al., 2014).

The different MCC contents (0.1 or 0.2%) decreased the typical starch intensity peak ($2\theta = 17^\circ$), similar to reported by Ma, Yu, & Kennedy (2005), which illustrated a restrained of the retrogradation of starch when cellulose fibers were added into the matrix. The decreased intensity of peaks at around $2\theta = 17^\circ$ was verified in films treated with MEF, which indicates a modification of crystalline region. This shows that, during the MEF treatment, a structure with a different X-ray diffraction pattern was developed. Similar results were found by Han, Zeng, Yu, Zhang, & Chen (2009) when applying pulsed electric fields (PEF). They observed a loss of crystallinity in the samples treated with 40 kV cm^{-1} showed by the decreased intensity of the peaks of the XRD spectra, indicating changes in the crystalline region.

No significant changes were observed in the FTIR spectra of chitosan-based films, indicating that cellulose microparticles were physically incorporated into chitosan in this method. Different intensities observed among the starch films suggests that the microparticles of cellulose physically added to the starch caused changes in the physical structure of the film. The influence of water content and crystallinity on starch samples was studied by Van Soest, Tournois, de Wit, & Vliegenthart (1995), that related these aspects with the 1000 cm^{-1} infrared band of the hydrogen bond of the C6 hydroxyl group, observing changes in the band with the addition of water. According to García et al. (2009), such results are due to C-OH flexural vibrations which are particularly sensitive to water content and are caused by changes in hydrogen bonding attributed to variations in the molecular environment of the primary hydroxyl group in amylose resulting from changes of intramolecular hydrogen bonding. In addition, both Van Soest et al. (1995) and García et al. (2009) also observed that the band intensity at 1022 cm^{-1} increases with decreasing crystallinity. The band reported by Van Soest et al. (1995) at 1022 cm^{-1} appears at 1012 cm^{-1} for all films, which shows differences between the spectra, with less intense peaks in the films ST.UB-0.2, ST.MEF-0.1 and ST.MEF-0.2. In these films, reflection peaks were attributed to the stronger cellulose crystallinity ($2\theta = 22.5$), as observed in the samples. XRD analyzes.

The peak values of thermal events for chitosan and starch-based films with MCC present four thermal events. The Peak 1 is related with the water evaporation process, a characteristic phenomenon of a polysaccharide with a hydrophilic nature; the Peak 2 (around 200 °C) attributed to the presence of glycerol; the Peak 3 (around 280 °C for the CH films and 300 °C for the ST film) related to polysaccharide decomposition (Cerqueira et al., 2012; Martins et al., 2012; Zohuriaan & Shokrolahi, 2004);

and the Peak 4 is attributed to the decomposition of the structures present in the cellulose observed in all samples with MCC, in the temperature range of 230–370 °C, which is the cleavage of glycoside linkages of the cellulose, leading to the formation of CO_2, H_2O, alkanes, and other hydrocarbon derivatives (Elanthikkal, Gopalakrishnapanicker, Varghese, & Guthrie, 2010).

The effect of MCC on thermal stability of CH and ST films was not completely evident. This is probably because the decomposition temperature of MCC occurs close to that of chitosan and starch. However, in starch films the incorporation of 0.1% MCC increases the thermal stability of the film, since there was an increase in the temperature of degradation and a significant decrease in weight loss ($p < 0.05$). This may be related to the good thermal stability of the crystalline structure for the MCC and good interaction between a reduced amount of MCC and starch. The starch control film treated with UB presented a peak of 309.53 ± 1.26 °C with a weight loss of $58.90.17 \pm 2.20$% while starch control film treated with MEF presented a peak of 308.35 ± 0.17 °C with a 49.58 ± 3.02 to weight loss, similar to the results obtained for other starches (Ma et al., 2008; Rico et al., 2016). The application of MEF showed no significant effect on the thermal stability of the films.

5. Conclusion

Chitosan or starch films reinforced with microcrystalline cellulose showed to be promising materials for the development of biodegradable composites. Also, the use of MEF showed to be a useful tool for the incorporation of MCC showing to have influence on the physical and structural properties of the films. The addition of MCC in chitosan films lead to more hydrophilic films, whereas for starch films the results showed a less hydrophilic behaviour. In this case the application of MEF was able to change this behaviour, since chitosan films with 0.1% MCC became hydrophobic ($\theta > 90°$), while starch films were even more hydrophilic ($\theta < 90°$). The higher concentration of MCC increased the opacity of the chitosan-based films and, in the same way, it significantly altered the mechanical properties of the films, generating more rigid films. SEM images showed morphological changes on the surface of the films, with more regular structure in chitosan films, whereas a more heterogeneous surface was found in starch films. The application of MEF showed no significant effect on the thermal stability of the film, but the addition of 0.1% MCC in starch films increased the thermal stability of the film significantly. In this sense the thermal properties of the films found in this study may increase their use as packaging materials in applications that high temperatures are needed.

The application of MEF as well as the addition of MCC are promising tools for the development of biodegradable chitosan or starch-based films.

Acknowledgments

The authors acknowledge Coordenação de Aperfeiçoamento Pessoal de Ensino Superior (CAPES), Embrapa Agroindústria de Alimentos (EMBRAPA) and Universidade do Minho for financial support. The authors also thank Dmitri Petrovykh from International Iberian Nanotechnology Laboratory for FTIR analytical support. The author Ricardo N. Pereira gratefully acknowledge to Portuguese Foundation for Science and Technology (FCT) its financial grant (SFRH/BPD/81887/2011).

Appendix A. Supplementary data

Supplementary data associated with this article can be found, in the online version, at http://dx.doi.org/10.1016/j.carbpol.2017.07.007.

References

Alparslan, Y., Baygar, T., Baygar, T., Hasanhocaoglu, H., & Metin, C. (2014). Effects of gelatin-based edible films enriched with laurel essential oil on the quality of rainbow trout (Oncorhynchus mykiss) fillets during refrigerated storage. *Food Technology and Biotechnology*, *52*(3), 325–333.

Azeredo, H. M. C., Mattoso, L. H. C., Wood, D., Williams, T. G., Avena-Bustillos, R. J., & McHugh, T. H. (2009). Nanocomposite edible films from mango puree reinforced with cellulose nanofibers. *Journal of Food Science*, *74*(5), 31–35. http://dx.doi.org/10.1111/j.1750-3841.2009.01186.x

Bondeson, D., Mathew, A., & Oksman, K. (2006). Optimization of the isolation of nanocrystals from microcrystalline cellulose by acid hydrolysis. *Cellulose*, *13*(2), 171–180. http://dx.doi.org/10.1007/s10570-006-9061-4

Casariego, A., Souza, B. W. S., Cerqueira, M. A., Teixeira, J. A., Cruz, L., Díaz, R., & Vicente, A. A. (2009). Chitosan/clay films' properties as affected by biopolymer and clay micro/nanoparticles' concentrations. *Food Hydrocolloids*, *23*(7), 1895–1902. http://dx.doi.org/10.1016/j.foodhyd.2009.02.007

Celebi, H., & Kurt, A. (2015). Effects of processing on the properties of chitosan/cellulose nanocrystal films. *Carbohydrate Polymers*, *133*, 284–293. http://dx.doi.org/10.1016/j.carbpol.2015.07.007

Cerqueira, M. A., Souza, B. W. S., Teixeira, J. A., & Vicente, A. A. (2012). Effect of glycerol and corn oil on physicochemical properties of polysaccharide films – A comparative study. *Food Hydrocolloids*, *27*(1), 175–184. http://dx.doi.org/10.1016/j.foodhyd.2011.07.007

Chuayjuljit, S., Su-Uthai, S., Tunwattanaseree, C., & Charuchinda, S. (2009). Preparation of microcrystalline cellulose from waste-cotton fabric for biodegradability enhancement of natural rubber sheets. *Journal of Reinforced Plastics and Composites*, *28*(10), 1245–1254. http://dx.doi.org/10.1177/0731684408089129

Cuq, B., Gontard, N., Cuq, J. L., & Guilbert, S. (1996). Functional properties of myofibrillar protein-based biopackaging as affected by film thickness. *Journal of Food Science*, *61*(3), 580–584. http://dx.doi.org/10.1111/j.1365-2621.1996.tb13163.x

Dehnad, D., Mirzaei, H., Emam-Djomeh, Z., Jafari, S. M., & Dadashi, S. (2014). Thermal and antimicrobial properties of chitosan-nanocellulose films for extending shelf life of ground meat. *Carbohydrate Polymers*, *109*, 148–154. http://dx.doi.org/10.1016/j.carbpol.2014.03.063

Eichhorn, S. J., Dufresne, A., Aranguren, M., Marcovich, N. E., Capadona, J. R., Rowan, S. J., & Peijs, T. (2010). Review: Current international research into cellulose nanofibres and nanocomposites. *Journal of Materials Science*, *45* http://dx.doi.org/10.1007/s10853-009-3874-0

Elanthikkal, S., Gopalakrishnapanicker, U., Varghese, S., & Guthrie, J. T. (2010). Cellulose microfibres produced from banana plant wastes: Isolation and characterization. *Carbohydrate Polymers*, *80*(3), 852–859. http://dx.doi.org/10.1016/j.carbpol.2009.12.043

Freire, C. S. R., Silvestre, A. J. D., Neto, C. P., Gandini, A., Martin, L., & Mondragon, I. (2008). Composites based on acylated cellulose fibers and low-density polyethylene: Effect of the fiber content, degree of substitution and fatty acid chain length on final properties. *Composites Science and Technology*, *68*(15–16), 3358–3364. http://dx.doi.org/10.1016/j.compscitech.2008.09.008

García, N. L., Famá, L., Dufresne, A., Aranguren, M., & Goyanes, S. (2009). A comparison between the physico-chemical properties of tuber and cereal starches. *Food Research International*, *42*(8), 976–982. http://dx.doi.org/10.1016/j.foodres.2009.05.004

Guillard, V., Broyart, B., Bonazzi, C., Guilbert, S., & Gontard, N. (2003). Preventing moisture transfer in a composite food using edible films: Experimental and mathematical study. *Journal of Food Science*, *68*(7), 2267–2277. http://dx.doi.org/10.1111/j.1365-2621.2003.tb05758.x

Han, Z., Zeng, X. A., Yu, S. J., Zhang, B. S., & Chen, X. D. (2009). Effects of pulsed electric fields (PEF) treatment on physicochemical properties of potato starch. *Innovative Food Science & Emerging Technologies*, *10*(4), 481–485. http://dx.doi.org/10.1016/j.ifset.2009.07.003

Khan, A., Khan, R. A., Salmieri, S., LeTien, C., Riedl, B., Bouchard, J., & Lacroix, M. (2012). Mechanical and barrier properties of nanocrystalline cellulose reinforced chitosan based nanocomposite films. *Carbohydrate Polymers*, *90*(4), 1601–1608. http://dx.doi.org/10.1016/j.carbpol.2012.07.037

Kwok, D. Y., & Neumann, A. W. (1999). Contact angle measurement and contact angle interpretation. *Advances in Colloid and Interface Science*, *81* http://dx.doi.org/10.1016/S0001-8686(98)00087-6

Lei, L., Zhi, H., Xiujin, Z., Takasuke, I., & Zaigui, L. (2007). Effects of different heating methods on the production of protein-lipid film. *Journal of Food Engineering*, *82*(3), 292–297. http://dx.doi.org/10.1016/j.jfoodeng.2007.02.030

Li, R., Fei, J., Cai, Y., Li, Y., Feng, J., & Yao, J. (2009). Cellulose whiskers extracted from mulberry: A novel biomass production. *Carbohydrate Polymers*, *76*(1), 94–99. http://dx.doi.org/10.1016/j.carbpol.2008.09.034

Li, D., Yang, N., Jin, Y., Zhou, Y., Xie, Z., Jin, Z., & Xu, X. (2016). Changes in crystal structure and physicochemical properties of potato starch treated by induced electric field. *Carbohydrate Polymers*, *153*, 535–541. http://dx.doi.org/10.1016/j.carbpol.2016.08.020

Lu, Y., Weng, L., & Cao, X. (2005). Biocomposites of plasticized starch reinforced with cellulose crystallites from cottonseed linter. *Macromolecular Bioscience*, *5*(11), 1101–1107. http://dx.doi.org/10.1002/mabi.200500094

Ma, X., Yu, J., & Kennedy, J. F. (2005). Studies on the properties of natural fibers-reinforced thermoplastic starch composites. *Carbohydrate Polymers*, *62*(1), 19–24. http://dx.doi.org/10.1016/j.carbpol.2005.07.015

Ma, X., Chang, P. R., & Yu, J. (2008). Properties of biodegradable thermoplastic pea starch/carboxymethyl cellulose and pea starch/microcrystalline cellulose composites. *Carbohydrate Polymers*, *72*(3), 369–375. http://dx.doi.org/10.1016/j.carbpol.2007.09.002

Ma, Q., Hu, D., Wang, H., & Wang, L. (2016). Tara gum edible film incorporated with oleic acid. *Food Hydrocolloids*, *56*, 127–133. http://dx.doi.org/10.1016/j.foodhyd.2015.11.033

Martins, J. T., Cerqueira, M. A., & Vicente, A. A. (2012). Influence of α-tocopherol on physicochemical properties of chitosan-based films. *Food Hydrocolloids*, *27*(1), 220–227. http://dx.doi.org/10.1016/j.foodhyd.2011.06.011

McHugh, T. H., Avenabustillos, R., & Krochta, J. M. (1993). Hydrophilic edible films-modified procedure for water-vapor permeability and explanation of thickness effects. *Journal of Food Science*, *58*(4), 899–903. http://dx.doi.org/10.1111/j.1365-2621.1993.tb09387.x

Pawlak, A., & Mucha, M. (2003). Thermogravimetric and FTIR studies of chitosan blends. *Thermochimica Acta*, *396*(1–2), 153–166. http://dx.doi.org/10.1016/S0040-6031(02)00523-3

Pereira, R. N., Souza, B. W. S., Cerqueira, M. A., Teixeira, J. A., & Vicente, A. A. (2010). Effects of electric fields on protein unfolding and aggregation: Influence on edible films formation. *Biomacromolecules*, *11*(11), 2912–2918. http://dx.doi.org/10.1021/bm100681a

Pereira, R. N., Rodrigues, R. M., Ramos, O. L., Xavier Malcata, F., Teixeira, J. A., & Vicente, A. A. (2016). Production of whey protein-based aggregates under ohmic heating. *Food and Bioprocess Technology*, *9*(4), 576–587. http://dx.doi.org/10.1007/s11947-015-1651-4

Reddy, J. P., & Rhim, J. W. (2014). Characterization of bionanocomposite films prepared with agar and paper-mulberry pulp nanocellulose. *Carbohydrate Polymers*, *110*, 480–488. http://dx.doi.org/10.1016/j.carbpol.2014.04.056

Rico, M., Rodríguez-Llamazares, S., Barral, L., Bouza, R., & Montero, B. (2016). Processing and characterization of polyols plasticized-starch reinforced with microcrystalline cellulose. *Carbohydrate Polymers*, *149*, 83–93. http://dx.doi.org/10.1016/j.carbpol.2016.04.087

Sastry, S. K., & Barach, J. T. (2000). Ohmic and inductive heating. *Journal of Food Science*, *65*(4), 42–46.

Segal, L., Creely, J. J., Martin, A. E., Jr, & Conrad, C. M. (1959). Empirical method for estimating the degree of crystallinity of native cellulose using the X-ray diffractometer. *Textile Research Journal*, 786–794.

Shankar, S., & Rhim, J. W. (2016). Preparation of nanocellulose from micro-crystalline cellulose: The effect on the performance and properties of agar-based composite films. *Carbohydrate Polymers*, *135*, 18–26. http://dx.doi.org/10.1016/j.carbpol.2015.08.082

Shi, A. M., Wang, L. J., Li, D., & Adhikari, B. (2013). Characterization of starch films containing starch nanoparticles Part 1: Physical and mechanical properties. *Carbohydrate Polymers*, *96*(2), 593–601. http://dx.doi.org/10.1016/j.carbpol.2012.12.042

Slavutsky, A. M., & Bertuzzi, M. A. (2014). Water barrier properties of starch films reinforced with cellulose nanocrystals obtained from sugarcane bagasse. *Carbohydrate Polymers*, *110*, 53–61. http://dx.doi.org/10.1016/j.carbpol.2014.03.049

Souza, B. W. S., Cerqueira, M. A., Casariego, A., Lima, A. M. P., Teixeira, J. A., & Vicente, A. A. (2009). Effect of moderate electric fields in the permeation properties of chitosan coatings. *Food Hydrocolloids*, *23*(8), 2110–2115. http://dx.doi.org/10.1016/j.foodhyd.2009.03.021

Souza, B. W. S., Cerqueira, M. A., Martins, J. T., Casariego, A., Teixeira, J. A., & Vicente, A. A. (2010). Influence of electric fields on the structure of chitosan edible coatings. *Food Hydrocolloids*, *24*(4), 330–335. http://dx.doi.org/10.1016/j.foodhyd.2009.10.011

SriBala, G., Chennuru, R., Mahapatra, S., & Vinu, R. (2016). Effect of alkaline ultrasonic pretreatment on crystalline morphology and enzymatic hydrolysis of cellulose. *Cellulose*, *23*(3), 1725–1740. http://dx.doi.org/10.1007/s10570-016-0893-2

Thoorens, G., Krier, F., Leclercq, B., Carlin, B., & Evrard, B. (2014). Microcrystalline cellulose, a direct compression binder in a quality by design environment – A review. *International Journal of Pharmaceutics*, *473*(1–2), 64–72. http://dx.doi.org/10.1016/j.ijpharm.2014.06.055

Tibolla, H., Pelissari, F. M., & Menegalli, F. C. (2014). Cellulose nanofibers produced from banana peel by chemical and enzymatic treatment. *LWT Food Science and Technology*, *59*(2P2), 1311–1318. http://dx.doi.org/10.1016/j.lwt.2014.04.011

Van Soest, J. J. G., Tournois, H., de Wit, D., & Vliegenthart, J. F. G. (1995). Short-range structure in (partially) crystalline potato starch determined with attenuated total reflectance Fourier-transform IR spectroscopy. *Carbohydrate Research*, *279(C*, 201–214. http://dx.doi.org/10.1016/0008-6215(95)00270-7

Zohuriaan, M. J., & Shokrolahi, F. (2004). Thermal studies on natural and modified gums. *Polymer Testing*, *23*(5), 575–579. http://dx.doi.org/10.1016/j.polymertesting.2003.11.001